

## New, thermodynamically consistent, integral equation for simple fluids

Forrest J. Rogers and David A. Young

Lawrence Livermore National Laboratory, University of California, Livermore, California 94550

(Received 31 January 1984)

A new integral equation in which the hypernetted-chain and Percus-Yevick approximations are "mixed" as a function of interparticle separation is described. An adjustable parameter  $\alpha$  in the mixing function is used to enforce thermodynamic consistency. For simple  $1/r^n$  potential fluids,  $\alpha$  is constant for all densities, and the solutions of the integral equations are in very good agreement with Monte Carlo calculations. For the one-component plasma,  $\alpha$  is a slowly varying function of density, but the agreement between calculated solutions and Monte Carlo is also good. This approach has definite advantages over previous thermodynamically consistent equations.

### I. INTRODUCTION

A number of recent papers<sup>1-5</sup> have attempted to improve the theory of classical fluids by imposing thermodynamic consistency on the solutions of integral equations such as the Percus-Yevick (PY) or hypernetted chain (HNC) equation. This is typically done by modifying the integral equation with a function which contains an adjustable parameter and then by varying this parameter until consistency is achieved. Consistency is obtained when the bulk modulus calculated from the virial equation ( $B_p$ ) is equal to that calculated from the compressibility equation ( $B_c$ ).

The advantage of this approach is that thermodynamic consistency leads to accurate radial-distribution-function solutions, apparently without regard to the details of the algorithm used. The principal disadvantage of the method is that it is computationally very time consuming. This is because the integral equation must be solved for each choice of the consistency parameter, and a number of iterations with this parameter are needed in order to achieve thermodynamic consistency. The consistency parameter must then be redetermined for each choice of density and temperature. This problem prevents routine use of the method for such applications as producing tables of distribution functions or computing the properties of multicomponent fluids.

In this paper we describe a new integral equation for which the consistency parameter is constant or slowly varying with fluid density for a spectrum of simple fluids. Once the parameter has been determined, the integral equation is equivalent to an HNC equation and can be solved very efficiently. Moreover, the solutions have been found to be in accurate agreement with Monte Carlo calculations.

In Sec. II we describe the new equation and the method of solution. In Sec. III we compare the solutions with Monte Carlo data for different pair potentials. In Sec. IV we discuss the results and possibilities for future research.

### II. NEW INTEGRAL EQUATION

For purely repulsive potentials, it is known<sup>1,2</sup> that the PY and HNC equations of state bracket the "exact"

Monte Carlo or molecular-dynamics computer simulation results. This suggests that some "mixture" of the two equations would yield an accurate equation of state. In addition, the bridge-diagram term which is omitted in the HNC equation is of short range only,<sup>3</sup> which suggests that the HNC approximation is appropriate for large interparticle distances and that the PY equation is more appropriate for small interparticle distances. Our algorithm combines these ideas.

The PY and HNC integral equations can be written

$$\gamma(r_{12}) = h(r_{12}) - c(r_{12}) = \rho \int c(r_{13}) h(r_{23}) dr_3, \quad (1)$$

which defines  $\gamma(r)$  and the direct correlation function  $c(r)$ , and

$$g(r) = \exp[-\beta u(r)][1 + \gamma(r)] \quad (\text{PY}) \quad (2)$$

or

$$g(r) = \exp[-\beta u(r)] \exp[\gamma(r)] \quad (\text{HNC}). \quad (3)$$

The  $h$  and  $g$  functions are related by  $h = g - 1$ .

The two approximations can be mixed in many ways, but we have found that

$$g(r) = \exp[-\beta u(r)] \left[ 1 + \frac{\exp[\gamma(r)f(r)] - 1}{f(r)} \right] \quad (4)$$

is a satisfactory algorithm. Here  $0 \leq f(r) \leq 1$ , with  $f(0) = 0$  and  $f(\infty) = 1$ . When  $r = 0$ ,  $f(0) = 0$ , and Eq. (4) reduces to the PY approximation. As  $r$  increases,  $f(r)$  approaches 1, and Eq. (4) reduces to the HNC approximation. We have chosen the simple mixing function

$$f(r) = 1 - \exp(-\alpha r), \quad (5)$$

where  $\alpha$  is the adjustable parameter used to achieve thermodynamic consistency. Equations (1), (4), and (5) together constitute what we call the thermodynamically consistent (TC) approximation. Our equation is similar in structure to the thermodynamically self-consistent equation of Hall and Conkie.<sup>4</sup>

A more fundamental justification for Eqs. (4) and (5) can be obtained diagrammatically. For hard spheres it is known<sup>6</sup> that the PY equation works fairly well because of a cancellation between certain convolution diagrams and

those bridge diagrams that are generated by adding one Mayer  $f$  bond to a convolution diagram. The result is that the  $y = \exp(\gamma)$  that occurs in the HNC equation is reduced to  $y = 1 + \gamma$ . The cancellation is due to the additional  $f$  bond being  $-1$  inside the hard-sphere diameter and zero outside. As not all bridge functions are canceled the PY equation is not exact and is thermodynamically inconsistent. For inverse  $n$ -power potentials a similar cancellation occurs, but it is not complete, and the resulting  $y$  function is intermediate between PY and HNC. Thus the mixing function  $f(r)$  should move toward 1 as  $n$  decreases. Also, for any given  $n$ ,  $f(r)$  should approach 1 as  $r$  increases because the bridge functions are short ranged. The function  $f(r)$  should not in fact be zero at  $r = 0$  since the uncanceled bridge functions make a substantial contri-

bution at  $r = 0$ . As a practical matter, however, the value of  $f(r)$  at small  $r$  has no effect on the TC result.

The numerical procedure used to solve Eqs. (1) and (4) is the same as described by Rogers.<sup>7</sup> We use dimensionless length units  $x = r/a$ , where  $a = (3/4\pi\rho)^{1/3}$  is the ion-sphere radius. For hard spheres and  $n = 18$  we used 2048 grid points and a step size  $\Delta x = 0.0125$ . For all other potentials we used 1024 grid points and a step size varying between 0.025 and 0.05. The extrapolation to  $\Delta x = 0$  described in Ref. 7 was used to improve the accuracy of the hard-sphere results. The parameter  $\alpha$  was determined by iteration at the freezing density until the two reduced moduli  $B_c$  and  $B_p$  were equal to within 0.5%. Typically, this required only two iterations.

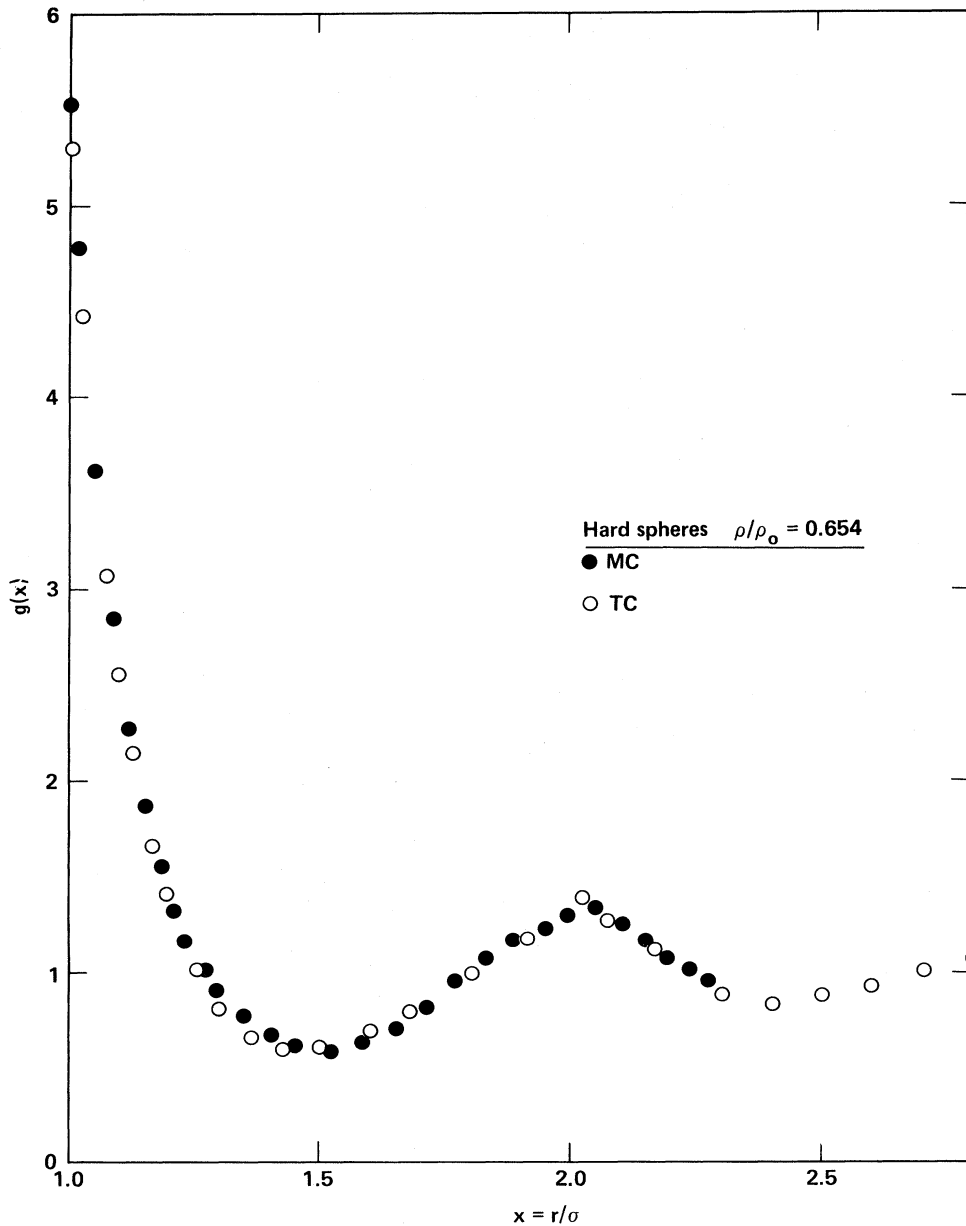


FIG. 1. Comparison of TC and MC  $g(x)$  for hard spheres at  $\rho/\rho_0 = 0.654$ .

TABLE I. Comparison of thermodynamically consistent ( $P_{TC}$ ) and Carnahan-Starling ( $P_{CS}$ ) excess reduced pressures for hard spheres. The CS pressures are a very accurate fit to molecular-dynamics data. The freezing point occurs at  $\rho/\rho_0=0.667$ .

| $\rho/\rho_0$ | $\eta$ | $P_{CS}$ | $pV/NkT - 1$ |                 |
|---------------|--------|----------|--------------|-----------------|
|               |        |          | $P_{TC}$     | $P_{TC}/P_{CS}$ |
| 0.10          | 0.074  | 0.359    | 0.359        | 1.000           |
| 0.20          | 0.148  | 0.887    | 0.884        | 0.997           |
| 0.30          | 0.222  | 1.678    | 1.664        | 0.992           |
| 0.40          | 0.296  | 2.895    | 2.850        | 0.984           |
| 0.50          | 0.370  | 4.832    | 4.714        | 0.976           |
| 0.60          | 0.444  | 8.055    | 7.781        | 0.966           |
| 0.654         | 0.484  | 10.707   | 10.294       | 0.961           |

### III. SOLUTIONS

The fluids we have chosen for analysis include the hard-sphere fluid, four inverse power potential fluids, and the one-component plasma. These fluids have in common the dependence of thermodynamic functions on only one coupling parameter.

#### A. Hard spheres

For hard spheres of diameter  $\sigma$  the appropriate coupling parameter is the relative density  $\rho/\rho_0$ , where  $\rho=N/V$  and  $\rho_0=\sqrt{2}/\sigma^3$  is the number density of hard spheres at closest packing. Another common parameter is the packing fraction  $\eta=(\pi\sqrt{2}/6)\rho/\rho_0$ .

The most severe test of the TC equation is to solve it at or near the freezing point, where the particles are most strongly correlated. Monte Carlo (MC) data<sup>8</sup> on

$g(x=r/\sigma)$  are available at  $\rho/\rho_0=0.654$ , which is very close to the freezing point<sup>9</sup> at  $\rho/\rho_0=0.667$ . The consistency parameter at  $\rho/\rho_0=0.654$  was found to be  $\alpha=0.16$ . The solution of the TC equation is compared to MC in Fig. 1. The equation of state has been computed for several densities and is compared with the Carnahan-Starling formula,<sup>10</sup> which is very nearly exact, in Table I. The same value of  $\alpha$  gives thermodynamic consistency at all densities.

#### B. Inverse power potentials

The general form of the inverse power potential is

$$u(r)=\epsilon\left[\frac{\sigma}{r}\right]^n, \quad (6)$$

where  $n$  can vary over the range  $3 < n < \infty$ . For this class of fluids, the coupling parameter<sup>11</sup> is  $z=(N\sigma^3/\sqrt{2}V)(\epsilon/kT)^{3/n}$ . In the dimensionless length units  $x=r/a$ , the interparticle potential appears as

$$u(x)=\frac{\Gamma}{x^n}, \quad (7)$$

where  $\Gamma=(4\pi\sqrt{2}z/3)^{n/3}$ .

A very useful list of MC  $g(x)$  data at the freezing point for the  $n=12, 9, 6$ , and 4 fluids has been published by Hansen and Schiff,<sup>12</sup> and we have used these data for direct comparison with our TC calculations. The MC equations of state over a range of  $z$  values and the freezing points for these fluids have been calculated by Hoover *et al.*<sup>11,13</sup> and by Hansen.<sup>14</sup>

At the freezing point for the  $1/r^{1/2}$  potential,  $z=0.813$ , and a MC  $g(x)$  is available at this point. Comparison of TC and MC  $g(x)$ 's is made in Fig. 2. The  $\alpha$

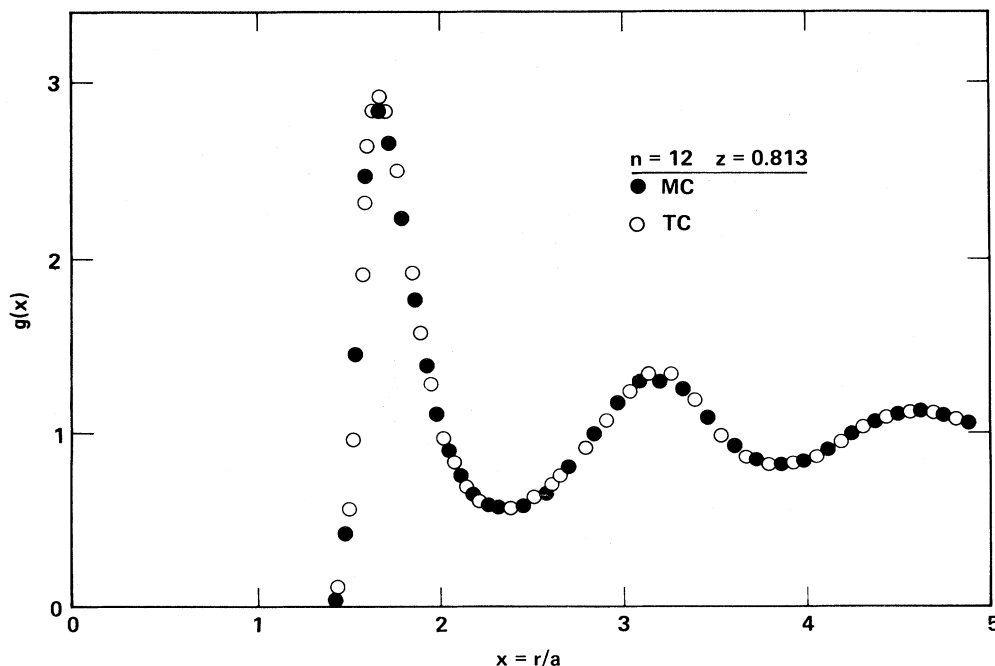


FIG. 2. Comparison of TC and MC  $g(x)$  for the inverse 12th-power fluid at  $z=0.813$ .

TABLE II. Comparison of thermodynamically consistent ( $P_{TC}$ ), Rosenfeld-Ashcroft ( $P_{RA}$ ), and Monte Carlo ( $P_{MC}$ ) excess reduced pressures for the inverse 12th-power fluid. The freezing point occurs at  $z=0.813$ .

| $z$   | $\Gamma$ | $P_{MC}$ | $pV/NkT-1$ |          |                 |
|-------|----------|----------|------------|----------|-----------------|
|       |          |          | $P_{RA}$   | $P_{TC}$ | $P_{TC}/P_{MC}$ |
| 0.10  | 0.123    | 0.448    |            | 0.449    | 1.002           |
| 0.20  | 1.970    | 1.121    |            | 1.121    | 1.000           |
| 0.30  | 9.975    | 2.101    |            | 2.109    | 1.004           |
| 0.40  | 31.52    | 3.557    | 3.547      | 3.536    | 0.994           |
| 0.50  | 76.96    | 5.641    |            | 5.562    | 0.986           |
| 0.60  | 159.6    | 8.460    |            | 8.392    | 0.992           |
| 0.70  | 295.7    | 12.469   | 12.36      | 12.283   | 0.985           |
| 0.813 | 538.0    | 18.7     |            | 18.360   | 0.982           |

value determined at  $z=0.813$  is 0.374, and the equation of state calculated with this number for lower densities is compared with MC in Table II. We have also carried out calculations with the thermodynamically consistent Rosenfeld-Ashcroft (RA) procedure,<sup>3</sup> and these results are also shown for comparison in Table II. In Table III the bulk moduli from the virial and compressibility equations are compared for the consistency parameter fixed at  $\alpha=0.374$ . The results show consistency for all  $z$  values.

In Fig. 3, TC and MC  $g(x)$ 's are compared at the freezing point,  $z=0.943$ , for the  $1/r^9$  potential. The TC and MC pressures are compared in Table IV for  $\alpha=0.499$ .

In Fig. 4, TC and MC  $g(x)$ 's are compared at the freezing point,  $z=1.54$ , for the  $1/r^6$  potential. The TC, RA, and MC pressures are compared in Table V for  $\alpha=0.750$ . In Table VI, the bulk moduli are compared at this  $\alpha$  value for various densities. Once again it is evident that consistency holds for constant  $\alpha$ .

TABLE III. Thermodynamic-consistency check for the inverse 12th-power fluid with  $\alpha=0.374$ .  $B_c$  and  $B_p$  are the reduced bulk moduli from the compressibility and virial equations, respectively.

| $z$   | $B_c$ | $B_p$ |
|-------|-------|-------|
| 0.10  | 2.00  | 2.00  |
| 0.20  | 3.74  | 3.74  |
| 0.30  | 6.63  | 6.64  |
| 0.40  | 11.25 | 11.27 |
| 0.50  | 18.40 | 18.39 |
| 0.60  | 29.08 | 29.05 |
| 0.70  | 44.57 | 44.59 |
| 0.813 | 69.78 | 70.14 |

In Fig. 5, TC and MC  $g(x)$ 's are compared at the freezing point,  $z=3.92$ , for the  $1/r^4$  potential. The TC, RA, and MC pressures are compared in Table VII. Because of the long range of this potential, the TC pressure must be corrected by adding a term  $2\Gamma/x_0$ , where  $x_0$  is the cutoff distance in the TC calculation. This additional term is included in the TC column of Table VII and amounts to a 1% correction.

The constancy of  $\alpha$  with varying coupling parameter was unexpected because previous papers on TC equations have shown consistency parameters which vary. Even more remarkable is the simple relationship between  $\alpha$  and  $n$ . In Fig. 6,  $\alpha$  is plotted against  $1/n$ , and for  $4 \leq n \leq 12$  it is accurately linear, given by  $\alpha=4.5/n$ . For  $n > 12$ , the curve deviates from a straight line and goes to the hard-sphere limit  $n = \infty$  at  $\alpha=0.160$ . The  $\alpha$  values are tabulated as a function of  $n$  in Table VIII.

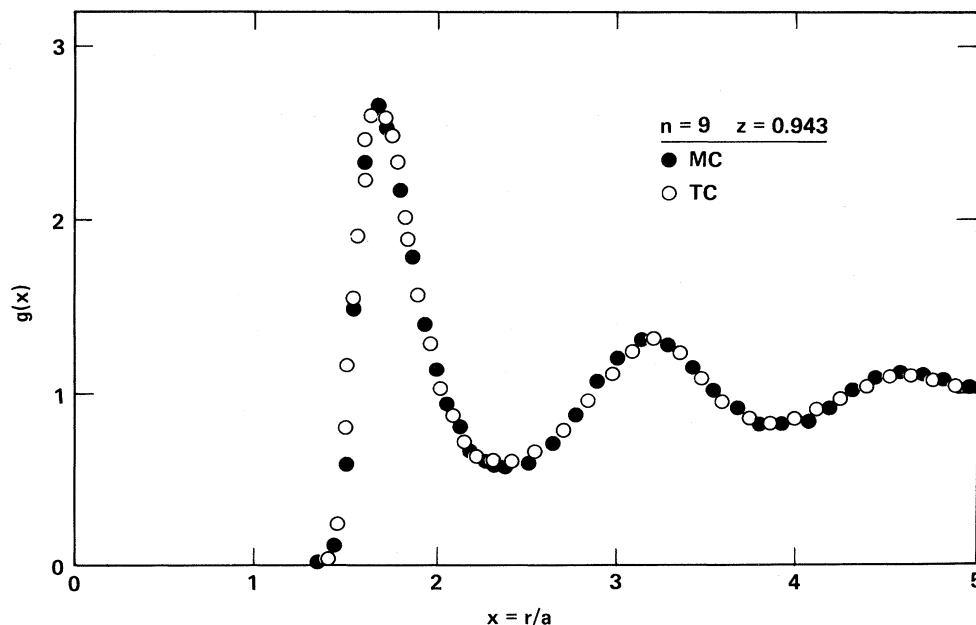


FIG. 3. Comparison of TC and MC  $g(x)$  for the inverse 9th-power fluid at  $z=0.943$ .

TABLE IV. Comparison of thermodynamically consistent ( $P_{TC}$ ) and Monte Carlo ( $P_{MC}$ ) excess reduced pressures for the inverse 9th-power fluid. The freezing point occurs at  $z=0.943$ .

| $z$   | $\Gamma$ | $pV/NkT-1$ |          |                 |
|-------|----------|------------|----------|-----------------|
|       |          | $P_{MC}$   | $P_{TC}$ | $P_{TC}/P_{MC}$ |
| 0.10  | 0.208    | 0.495      | 0.496    | 1.002           |
| 0.25  | 3.248    | 1.701      | 1.701    | 1.000           |
| 0.50  | 25.98    | 5.598      | 5.548    | 0.991           |
| 0.943 | 174.3    | 21.9       | 21.943   | 1.002           |

### C. One-component plasma

The one-component plasma (OCP) fluid consists of ions of charge  $+Ze$  moving in a negative neutralizing background of constant density. The OCP is nominally a  $1/r$  potential fluid, but it differs from the other inverse power fluids in that a neutralizing background is needed to cancel the long-range Coulomb potential between the ions. The OCP coupling parameter is  $\Gamma=(Ze)^2/kTa$ . This system has been extensively studied, and accurate Monte Carlo  $g(x)$  and equation-of-state data<sup>15</sup> are available.

We have found that the consistency parameter  $\alpha$  is not a constant as  $\Gamma$  changes, and that by setting

$$f(r)=[1-\exp(-ar)]^m, \quad (8)$$

we can improve the agreement between the MC and TC equation of state by increasing  $m$  to 10. The function  $f(r)$  significantly affects the TC solutions only in the region  $1.3 \leq x \leq 2$ , and adjustment of the power  $m$  allows us to change the shape of  $f(r)$  in this region. We have found that for  $n \geq 4$ ,  $m=1$  gives the best agreement with MC data. Also, the consistency shown in Tables III and VI for  $n=12$  and 6 is best for  $m=1$ .

TABLE V. Comparison of thermodynamically consistent ( $P_{TC}$ ), Rosenfeld-Ashcroft ( $P_{RA}$ ), and Monte Carlo ( $P_{MC}$ ) excess reduced pressures for the inverse 6th-power fluid. The freezing point occurs at  $z=1.54$ .

| $z$  | $\Gamma$ | $pV/NkT-1$ |          |          |                 |
|------|----------|------------|----------|----------|-----------------|
|      |          | $P_{MC}$   | $P_{RA}$ | $P_{TC}$ | $P_{TC}/P_{MC}$ |
| 0.10 | 0.351    | 0.638      |          | 0.639    | 1.002           |
| 0.25 | 2.193    | 2.056      |          | 2.049    | 0.997           |
| 0.50 | 8.773    | 5.686      | 5.672    | 5.669    | 0.997           |
| 1.00 | 35.09    | 17.932     | 17.886   | 17.950   | 1.001           |
| 1.54 | 83.22    | 38.8       |          | 39.028   | 1.006           |

In Fig. 7, TC, RA, and MC  $g(x)$ 's are compared at  $\Gamma=170$ , which is close to the freezing point,<sup>15</sup>  $\Gamma=178$ . The TC, RA, and MC pressures are compared in Table IX.

One of the best procedures for obtaining thermodynamic consistency is due to Rosenfeld and Ashcroft.<sup>3</sup> They assume that to a good approximation the hard-sphere bridge functions form a universal set and that, except for a density shift, and PY hard-sphere bridge functions have the same functional form as the true bridge functions. In our TC method, by mixing the PY and HNC equations, we have also introduced the PY bridge functions, but now for the actual potential being treated, thus removing reliance on the assumption of universality. It is therefore of some interest to compare the bridge functions predicted by the TC method with the RA hard-sphere function.

The exact  $g(r)$  is given in terms of the bridge functions  $B(r)$  by

$$g(r)=\exp[-\beta u(r)]\exp[\gamma(r)-B(r)]. \quad (9)$$

Using Eqs. (4) and (9), we can solve for  $B(r)$ :

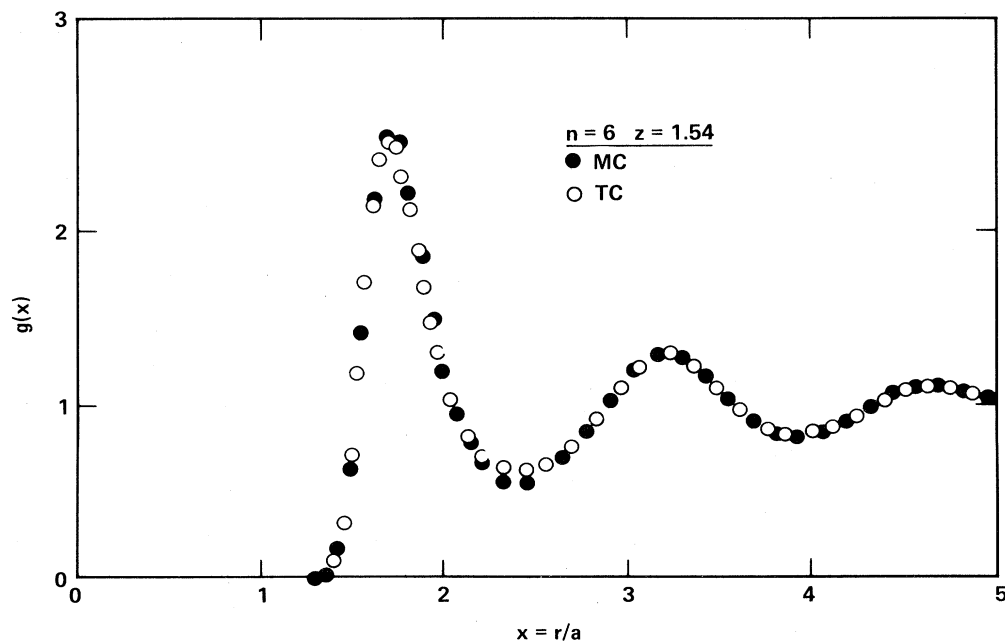


FIG. 4. Comparison of TC and MC  $g(x)$  for the inverse 6th-power fluid at  $z=1.54$ .

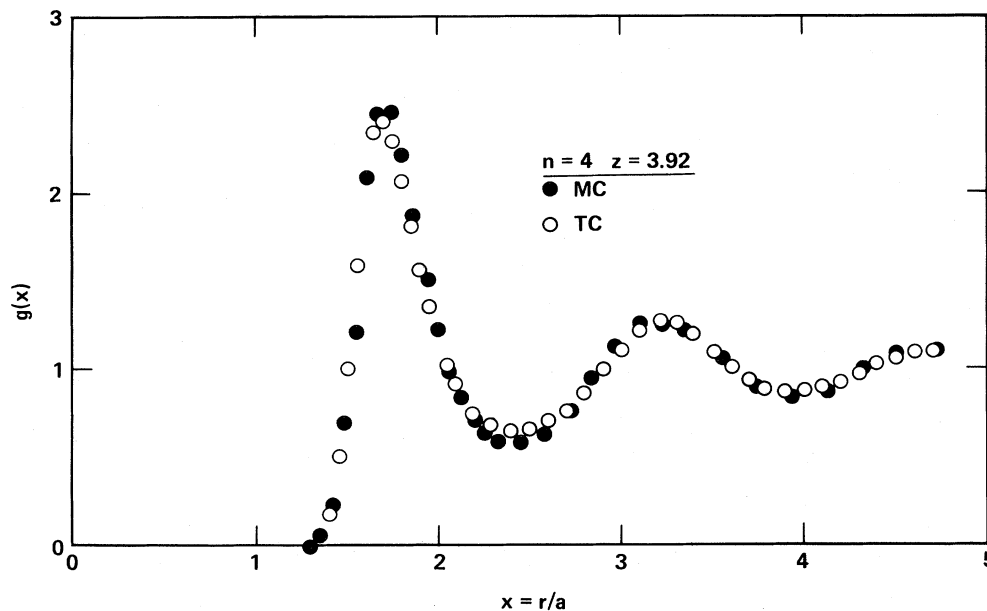


FIG. 5. Comparison of TC and MC  $g(x)$  for the inverse 4th-power fluid at  $z = 3.92$ .

$$B(r) = \gamma(r) - \ln \left[ 1 + \frac{\exp[\gamma(r)f(r)] - 1}{f(r)} \right]. \quad (10)$$

In Fig. 8 we compare the TC and RA bridge functions for hard spheres at  $\rho/\rho_0 = 0.5657$ . In the region of the first peak the two functions are almost coincident. Beyond the first zero in  $B(x)$ , corresponding to  $g(x) = 1$ , the magnitude of  $B(x)$  is shown amplified by a factor of 10. Even here the two methods give similar results. Although it has almost no effect on the thermodynamics, the tail of  $B(x)$  does depend strongly on the potential, and the universality assumption fails. For example, for the OCP, the TC  $B(x)$  shows no oscillations at large  $x$ , while the RA  $B(x)$  is constrained to show the hard-sphere oscillations. In Fig. 8 we also show  $\gamma(x)$ , and it is clear that  $B(x)$  varies as  $[\gamma(x)]^2$  to lowest order.

#### IV. DISCUSSION

A glance at the figures shows that the solutions of the TC equation are in good, if not excellent, agreement with MC results. The largest discrepancies appear in  $g(x)$  at the first peak and first minimum, and are most noticeable for  $n = 4$ . The calculated TC pressures, on the other hand, are in worst agreement with MC for hard spheres

TABLE VI. Thermodynamic-consistency check for the inverse 6th-power fluid with  $\alpha = 0.750$ .  $B_c$  and  $B_p$  are the reduced bulk moduli from the compressibility and virial equations, respectively.

| $z$  | $B_c$  | $B_p$  |
|------|--------|--------|
| 0.10 | 2.39   | 2.39   |
| 0.25 | 5.85   | 5.85   |
| 0.50 | 15.55  | 15.48  |
| 1.00 | 50.51  | 50.19  |
| 1.54 | 110.96 | 111.04 |

and then improve with decreasing  $n$ , as indicated in the tables. The reason for this apparent discrepancy is that for large  $n$  the pressure is very sensitive to the details of  $g(x)$  near the first peak, and small errors in  $g(x)$  there are amplified to large errors in the pressure.

Hall and Conkie<sup>4</sup> have described a parametrized, thermodynamically consistent method that in the case of hard spheres gives results superior to those of the current approach. Their method truncates the expansion of  $g(r)$  in powers of  $\gamma(r)$  at the quadratic term according to

$$g(r) = \exp[-\beta u(r)] \{ 1 + \gamma(r) + [a(\rho) + b(\rho)f(r)][\gamma(r)]^2 \}, \quad (11)$$

where  $a(\rho)$  and  $b(\rho)$  are density-dependent parameters determined from the requirement of thermodynamic consistency and  $f(r) = r$ . It is well known that for hard

TABLE VII. Comparison of thermodynamically consistent ( $P_{TC}$ ), Rosenfeld-Ashcroft ( $P_{RA}$ ), and Monte Carlo ( $P_{MC}$ ) excess reduced pressures for the inverse 4th-power fluid. The TC values have been corrected for the long-range potential tail. The freezing point occurs at  $z = 3.92$ .

| $z$  | $\Gamma$ | $pV/NkT - 1$ |          |          | $P_{TC}/P_{MC}$ |
|------|----------|--------------|----------|----------|-----------------|
|      |          | $P_{MC}$     | $P_{RA}$ | $P_{TC}$ |                 |
| 0.10 | 0.498    | 1.225        |          | 1.222    | 0.998           |
| 0.25 | 1.688    | 3.467        |          | 3.455    | 0.996           |
| 0.50 | 4.254    | 7.889        | 7.897    | 7.895    | 1.001           |
| 1.00 | 10.72    | 18.640       |          | 18.631   | 1.000           |
| 1.50 | 18.40    | 31.120       | 31.075   | 31.161   | 1.001           |
| 2.00 | 27.01    | 44.947       |          | 45.070   | 1.003           |
| 2.50 | 36.36    | 59.853       | 59.866   | 60.113   | 1.004           |
| 3.00 | 46.38    | 75.853       |          | 76.155   | 1.004           |
| 3.50 | 56.96    | 92.747       |          | 93.064   | 1.003           |
| 3.92 | 66.25    | 107.7        |          | 107.879  | 1.002           |

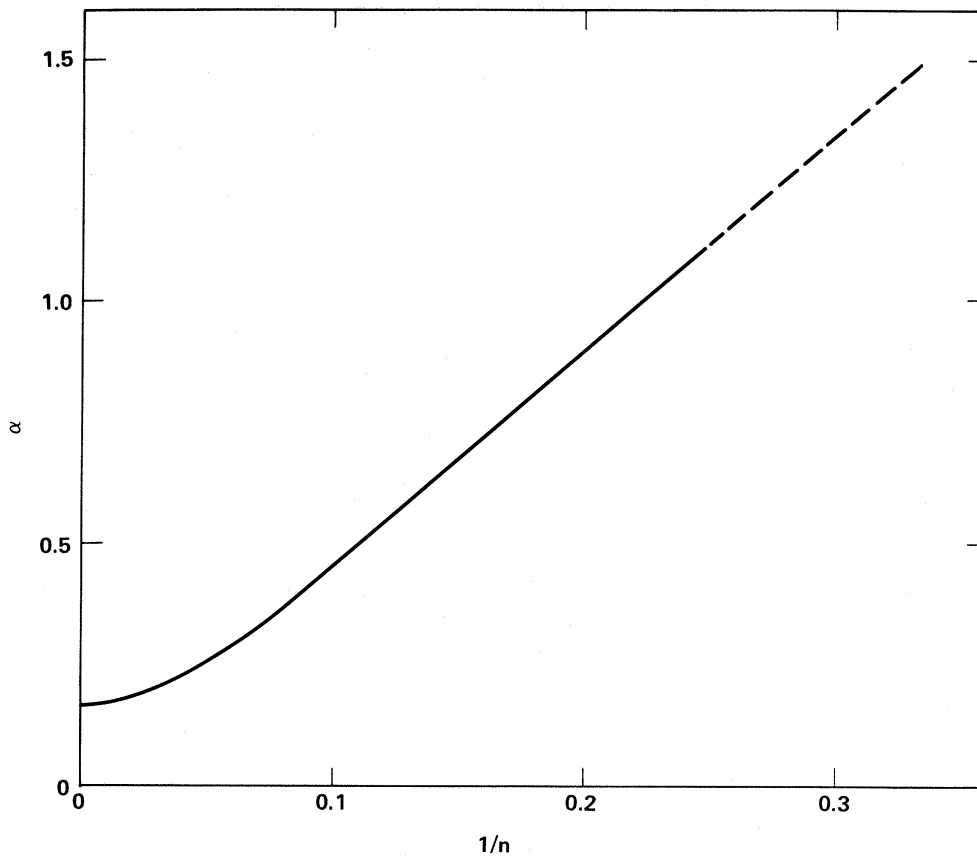


FIG. 6. Consistency parameter  $\alpha$  as a function of  $1/n$  for inverse  $n$ -power fluids.

spheres, truncation of  $g(r)$  at the linear term (PY equation) gives fairly good results. The success of the Hall and Conkie procedure is apparently due to a very accurate approximation to the true quadratic term and to the fact that the cubic and higher-order terms are small. Applica-

tion of this method to the inverse 12th-power potential was less successful.<sup>4</sup> This is to be expected since the range of  $r$  over which  $\exp[\gamma(r)] \gg 1$  increases as the range of the potential increases and the expansion used in Eq. (11) becomes inadequate. By adding more terms to Eq. (11)

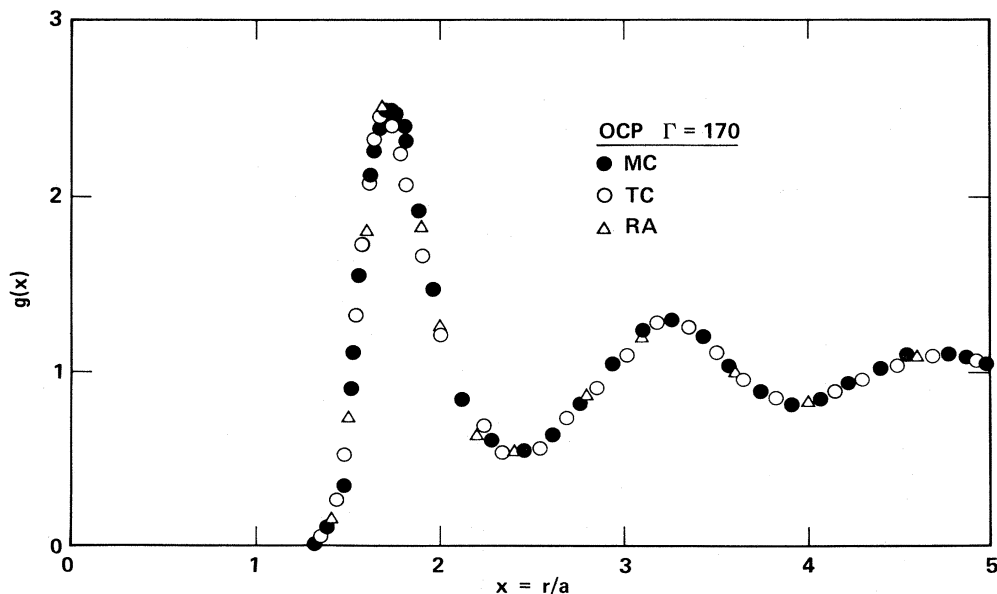


FIG. 7. Comparison of TC, RA, and MC  $g(x)$  for the OCP at  $\Gamma=170$ .

TABLE VIII. Consistency parameter  $\alpha$  for the inverse  $n$ -power fluids.

| $n$      | $\alpha$ |
|----------|----------|
| 4        | 1.113    |
| 6        | 0.750    |
| 9        | 0.499    |
| 12       | 0.374    |
| 18       | 0.263    |
| $\infty$ | 0.160    |

the expansion could in principle be extended to longer-ranged potentials, but this has not yet been attempted.

The RA scheme gives better accuracy than the TC in thermodynamic functions for hard spheres and the OCP, and comparable accuracy for the other fluids. It deviates from the correct hard-sphere pressure at melting by about 2% and is nearly exact for the OCP.<sup>16</sup> The main problem with RA is that it is very time consuming to calculate

TABLE IX. Comparison of thermodynamically consistent ( $P_{TC}$ ), Rosenfeld-Ashcroft ( $P_{RA}$ ), and Monte Carlo ( $P_{MC}$ ) excess reduced pressures for the one-component plasma. The freezing point occurs at  $\Gamma=178$ .

| $\Gamma$ | $pV/NkT - 1$ |          |          | $P_{TC}/P_{MC}$ | $\alpha$ |
|----------|--------------|----------|----------|-----------------|----------|
|          | $P_{MC}$     | $P_{RA}$ | $P_{TC}$ |                 |          |
| 20       | -5.558       | -5.559   | -5.568   | 1.002           | 4.510    |
| 50       | -14.367      | -14.368  | -14.365  | 1.000           | 4.225    |
| 100      | -29.174      | -29.175  | -29.157  | 0.999           | 4.050    |
| 140      | -41.033      |          | -41.030  | 1.000           | 3.985    |
| 170      | -49.999      | -49.992  | -49.942  | 0.999           | 3.963    |

solutions. A new variational parameter is needed for each density point, and the computer time required for convergence increases dramatically near the freezing point. The RA method is thus impractical for routine calculation of distribution functions and for multicomponent system calculations. The present TC model is, because of the constant or slowly varying  $\alpha$ , about an order of magnitude

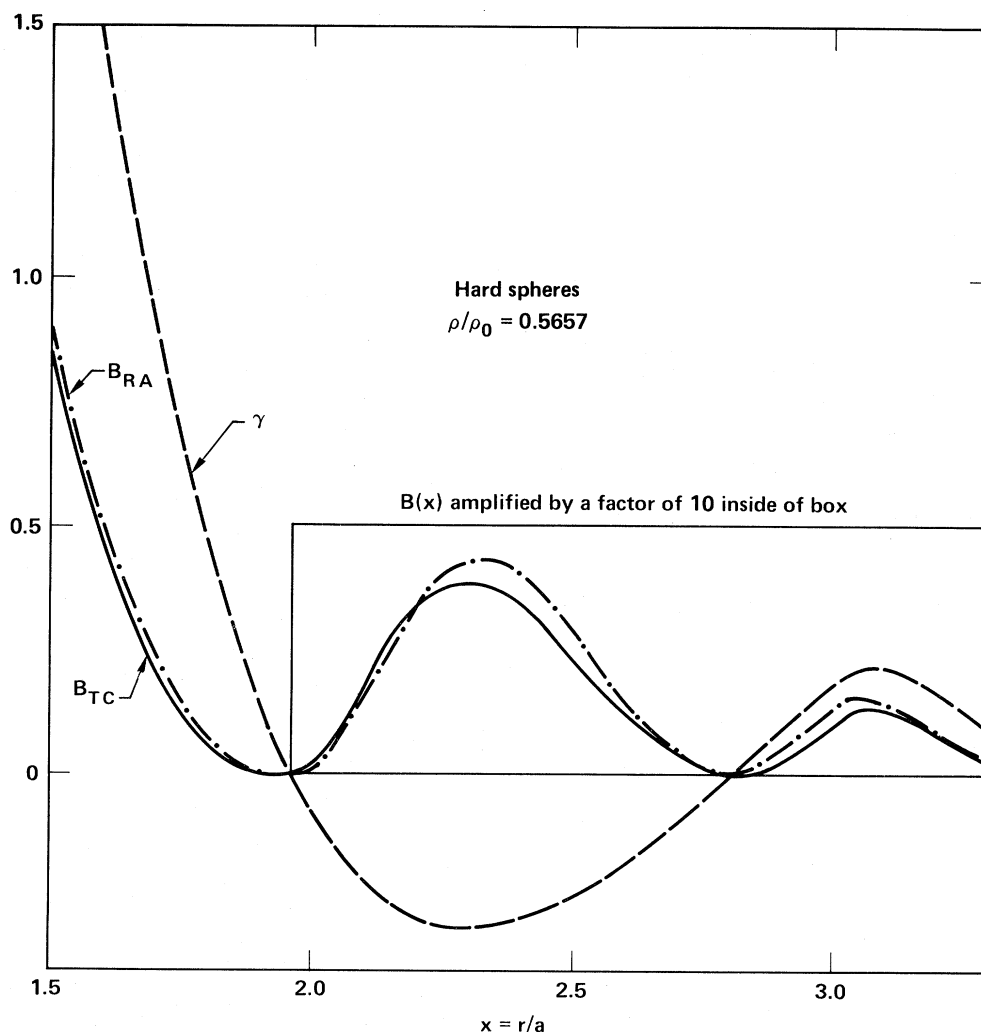


FIG. 8. Comparison of the TC and RA bridge functions for hard spheres at  $\rho/\rho_0=0.5657$  ( $\eta=0.4189$ ). The RA bridge function is calculated at  $\eta'=0.3767$ . The function  $\gamma(x)$  is shown for comparison.

faster than RA when generating tables. Preliminary studies show that it is suitable for multicomponent system calculations and that it can be used for fast generation of  $g(x)$  tables for use in fluid perturbation-theory calculations.

It is evident to us that our choice of the mixing function  $f(x)$  is arbitrary and not necessarily optimal. Other simple functions might yield improved solutions with no extra computational effort. Also, the constancy of  $\alpha$  with density and the very simple form of  $\alpha$  as a function of  $n$

suggest that a deeper physical explanation may be available for the success of the TC method described here.

#### ACKNOWLEDGMENTS

We thank H. E. DeWitt and W. G. Hoover for valuable discussions. This work was performed under the auspices of the U. S. Department of Energy by Lawrence Livermore National Laboratory under Contract No. W-7405-Eng-48 and supported in part by the U.S. Office of Naval Research.

---

<sup>1</sup>P. Hutchinson and W. R. Conkie, *Mol. Phys.* **21**, 881 (1971).

<sup>2</sup>P. Hutchinson and W. R. Conkie, *Mol. Phys.* **24**, 567 (1972).

<sup>3</sup>Y. Rosenfeld and N. V. Ashcroft, *Phys. Rev. A* **20**, 1208 (1979).

<sup>4</sup>D. S. Hall and W. R. Conkie, *Mol. Phys.* **40**, 907 (1980).

<sup>5</sup>L. Verlet, *Mol. Phys.* **42**, 1291 (1981).

<sup>6</sup>P. A. Egelstaff, *An Introduction to the Liquid State* (Academic, London, 1967), pp. 57 and 58.

<sup>7</sup>F. J. Rogers, *J. Chem. Phys.* **73**, 6272 (1980).

<sup>8</sup>J. A. Barker and D. Henderson, *Annu. Rev. Phys. Chem.* **23**, 439 (1972).

<sup>9</sup>W. G. Hoover and F. H. Ree, *J. Chem. Phys.* **49**, 204 (1968).

<sup>10</sup>N. F. Carnahan and K. E. Starling, *J. Chem. Phys.* **51**, 635 (1969).

<sup>11</sup>W. G. Hoover, S. G. Gray, and K. W. Johnson, *J. Chem. Phys.* **55**, 1128 (1971).

<sup>12</sup>J.-P. Hansen and D. Schiff, *Mol. Phys.* **25**, 1281 (1973).

<sup>13</sup>W. G. Hoover, M. Ross, K. W. Johnson, D. Henderson, J. A. Barker, and B. C. Brown, *J. Chem. Phys.* **52**, 4931 (1970).

<sup>14</sup>J.-P. Hansen, *Phys. Rev. A* **2**, 221 (1970).

<sup>15</sup>W. L. Slattery, G. D. Doolen, and H. E. DeWitt, *Phys. Rev. A* **26**, 2255 (1982).

<sup>16</sup>F. J. Rogers, D. A. Young, H. E. DeWitt, and M. Ross, *Phys. Rev. A* **28**, 2990 (1983).